

# Characterization of lead glazed potteries from Smyrna (Izmir/Turkey) using multiple analytical techniques; Part I: Glaze and engobe

M. Özçatal<sup>a</sup>, M. Yaygingöl<sup>c</sup>, A. İssi<sup>b,\*</sup>, A. Kara<sup>c</sup>, S. Turan<sup>c</sup>, F. Okyar<sup>c</sup>, Ş. Pfeiffer Taş<sup>c</sup>, I. Nastova<sup>d</sup>,  
O. Grupče<sup>d</sup>, B. Minčeva-Šukarova<sup>d</sup>

<sup>a</sup>Afyon Kocatepe University, Faculty of Technology, Department of Metallurgical and Materials Engineering, Afyonkarahisar, Turkey

<sup>b</sup>Dumlupınar University, Department of Materials Science and Engineering, Kütahya, Turkey

<sup>c</sup>Anadolu University, Department of Materials Science and Engineering, Eskişehir, Turkey

<sup>d</sup>Ss. Cyril and Methodius University, Institute of Chemistry, Faculty of Natural Sciences and Mathematics, POB 162, 1001 Skopje, Republic of Macedonia

Received 14 June 2013; received in revised form 3 September 2013; accepted 4 September 2013

Available online 13 September 2013

## Abstract

Eighteen lead glazed potsherds from the Ayasuluk region (Smyrna) were characterized in order to have detailed knowledge of their production technology. Micro-Raman and scanning electron microscopy (SEM) with the combination of an energy dispersive X-ray spectrometer (EDX) was used for their characterization. EDX analysis of the glaze layers showed that lead oxide was used as a fluxing agent for the production of most of the potsherds. Microstructural characteristics such as rod-shaped crystals at the interaction layers, residual quartz crystals inside the glaze layers and coloration of the decorations of the potsherds were also evaluated in the study. Furthermore, micro-Raman spectra provided bases for evaluation of firing temperature of the glazes based on the polymerization index ( $I_p$ ) values. The low  $I_p$  values, for all of the analyzed samples (except for two of them), indicated that the glazes were rich in lead oxide and should have been fired at temperatures below 700 °C. In the Raman spectra of the glazes, several pigments and/or colored minerals were identified: These were namely lead white, anatase, quartz, calcite, red ochre, lazurite and carbon black.

© 2013 Elsevier Ltd and Techna Group S.r.l. All rights reserved.

**Keywords:** Archaeometrical characterization; Lead glazed pottery; Raman spectra of glazes; İzmir

## 1. Introduction

One of the favorite ceramics produced during the Middle Ages in Anatolia was lead glazed potteries. Ottoman and Byzantine cultures occupied similar characteristics for the production of these potteries. They were produced in different places in Anatolia such as Tarsus, İznik, Smyrna, Clazomenae, Ephesus and Perge [1–4]. The ease of production of such wares at relatively low temperatures with the desired transparency and

bright colored glazes were the main reasons for their preference [5]. Therefore, it was one of the important groups of ceramic wares for the Late Hellenistic, Roman, Byzantine and Ottoman cultures in Anatolia [1,2]. Archaeological excavations have brought to light some lead glazed potsherds at the Ayasuluk region in İzmir dated back to the fifteenth–seventeenth centuries occupied by Byzantine and Ottoman cultures.

Scanning electron microscopy (SEM) with an energy dispersive X-ray spectrometer (EDX) and micro-Raman analysis are useful characterization techniques to determine the elemental and mineralogical composition, identification of pigments and polymerization indexes of the glaze layer of the potsherds. The main purpose of this study was to determine elemental compositions, key elements used for pigments or colorant agents and estimation of firing temperatures reached

\*Correspondence to: Dumlupınar University, Faculty of Engineering, Department of Materials Science and Engineering, Evliya Celebi Campus, 43100 Kutahya, Turkey. Tel.: +90 274 265 2031x4309; fax: +90 274 265 2066

E-mail address: [aliissi@hotmail.com](mailto:aliissi@hotmail.com) (A. İssi).

Table 1  
Representative optical images and macro descriptions of the investigated lead glazed potsherds.

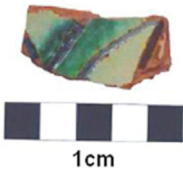


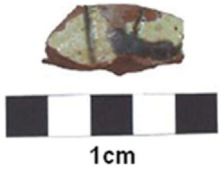
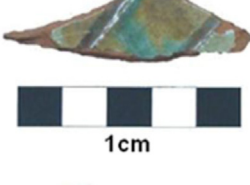
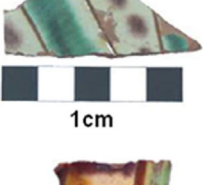

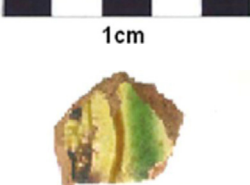

Sample code	Macro descriptions	Images
G1	Sgraffito, green glaze, white engobe, red body fragment	
G2	Sgraffito, yellow-green glaze, white engobe, red body fragment	
G3	Sgraffito, yellow-green glaze, white engobe, red body fragment	
G4	Sgraffito, beige-brown glaze, white engobe, red body fragment	
G5	Sgraffito, aqua blue glaze, white engobe, red body fragment	
G6	Sgraffito, green-brown glaze, white engobe, red body fragment	
G7	Sgraffito, yellow-green glaze, white engobe, red body fragment	
G8	Sgraffito, yellow glaze, white engobe, red body fragment	
G9	Sgraffito, yellow-green glaze, white engobe, red body fragment	

Table 1 (continued)

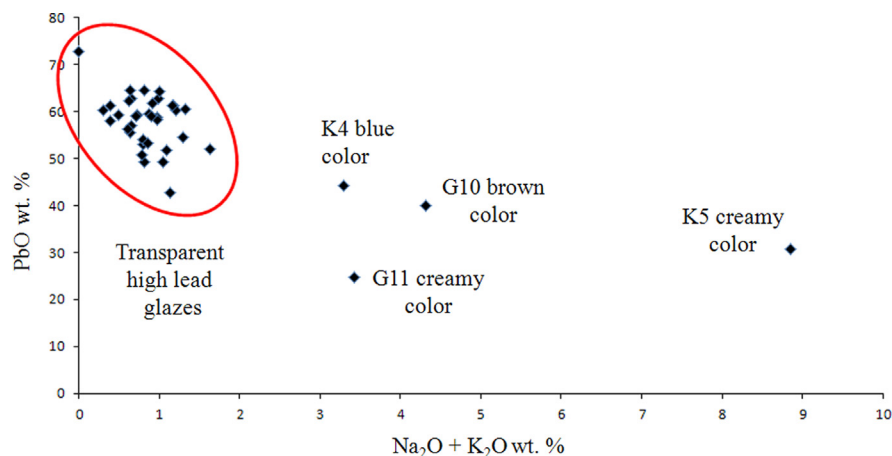
Sample code	Macro descriptions	Images
G10	Sgraffito, green glaze, white engobe, red body fragment	
G11	Sgraffito, beige glaze, white engobe, red body fragment	
G12	Sgraffito, dark green glaze, white engobe, red body fragment	
K1	Monochromatic green glaze, dark beige engobe, red body fragment	
K2	Damaged green glaze, rose-beige engobe, red body fragment	
K3	Damaged green glaze, rose-beige engobe, red body fragment, over fired	
K4	Monochromatic blue and green glaze, body red fragment	
K5	Miletus ware, dark blue-beige glaze, white engobe, red body fragment	
K6	Yellow-green glaze, white engobe, red body fragment	

Table 2

Semi-quantitative EDX results of the glaze layers and decorations (wt%).

Sample code	Color	SiO <sub>2</sub>	Al <sub>2</sub> O <sub>3</sub>	PbO	Na <sub>2</sub> O	K <sub>2</sub> O	CaO	MgO	Fe <sub>2</sub> O <sub>3</sub>	TiO <sub>2</sub>	P <sub>2</sub> O <sub>5</sub>	CuO	MnO	SnO <sub>2</sub>
G1	brown (graffito)	28.66	5.51	59.16	0.24	0.49	0.78	n.d.	5.11	n.d.	n.d.	n.d.	n.d.	n.d.
G1	green (graffito)	28.51	6.28	61.32	0.44	0.74	1.11	0.45	1.15	n.d.	n.d.	n.d.	n.d.	n.d.
G1	pale green	29.74	11.65	53.03	n.d.	0.80	0.89	0.80	2.10	n.d.	n.d.	0.99	n.d.	n.d.
G2	brown (graffito)	32.99	5.14	54.41	0.38	0.92	0.79	0.79	3.10	n.d.	n.d.	1.49	n.d.	n.d.
G2	brown	31.88	8.82	53.99	n.d.	0.80	0.56	0.61	1.89	n.d.	n.d.	n.d.	n.d.	n.d.
G2	green	37.32	5.10	53.23	n.d.	0.86	0.73	0.65	1.51	n.d.	n.d.	0.61	n.d.	n.d.
G3	brown (graffito)	38.13	5.33	51.79	0.28	0.82	0.78	0.55	2.28	n.d.	n.d.	n.d.	n.d.	n.d.
G3	yellow	40.50	5.94	49.22	0.28	0.77	0.90	0.56	1.83	n.d.	n.d.	n.d.	n.d.	n.d.
G3	green	40.55	5.95	49.16	n.d.	0.82	0.60	0.55	1.08	n.d.	n.d.	1.58	n.d.	n.d.
G4	brown (graffito)	27.83	5.24	60.61	n.d.	1.32	1.65	0.69	2.68	n.d.	n.d.	n.d.	n.d.	n.d.
G4	creamy white	33.13	3.70	59.03	0.43	0.48	1.33	0.70	1.20	n.d.	n.d.	n.d.	n.d.	n.d.
G5	green	24.98	2.13	72.89	n.d.	n.d.	n.d.	n.d.	n.d.	n.d.	n.d.	n.d.	n.d.	n.d.
G6	brown (graffito)	28.64	3.89	64.51	0.56	0.25	0.51	0.39	1.26	n.d.	n.d.	n.d.	n.d.	n.d.
G6	yellow	32.62	3.97	61.36	0.53	0.63	0.45	0.43	n.d.	n.d.	n.d.	n.d.	n.d.	n.d.
G6	green	31.34	2.76	60.41	n.d.	0.31	0.54	0.34	0.37	n.d.	n.d.	3.94	n.d.	n.d.
G7	brown (graffito)	25.67	5.49	64.63	n.d.	0.64	0.86	0.66	2.06	n.d.	n.d.	n.d.	n.d.	n.d.
G7	yellow	28.25	5.25	61.76	0.42	0.50	0.64	0.35	2.12	n.d.	n.d.	0.72	n.d.	n.d.
G8	brown (graffito)	32.59	3.27	61.41	n.d.	0.39	0.45	0.33	1.56	n.d.	n.d.	n.d.	n.d.	n.d.
G8	yellow-green	32.16	2.91	62.21	n.d.	0.62	0.76	0.48	0.87	n.d.	n.d.	n.d.	n.d.	n.d.
G9	brown	25.59	9.35	58.05	n.d.	0.40	1.00	0.39	5.22	n.d.	n.d.	n.d.	n.d.	n.d.
G9	green	27.89	2.31	64.41	0.48	0.53	1.77	0.33	2.29	n.d.	n.d.	n.d.	n.d.	n.d.
G10	brown (graffito)	38.83	7.71	40.03	1.11	3.20	2.38	1.51	3.16	n.d.	2.01	n.d.	n.d.	n.d.
G10	brown	34.52	3.63	55.41	n.d.	0.64	1.61	0.45	0.72	n.d.	n.d.	n.d.	3.03	n.d.
G10	pale green	34.29	6.31	56.40	n.d.	0.61	1.04	0.54	0.83	n.d.	n.d.	n.d.	n.d.	n.d.
G11	brown	44.15	6.75	42.80	n.d.	1.13	1.15	1.57	2.22	n.d.	n.d.	n.d.	n.d.	n.d.
G11	creamy	59.32	9.32	24.67	0.90	2.53	0.84	0.78	1.65	n.d.	n.d.	n.d.	n.d.	n.d.
G12	green (graffito)	31.25	2.60	62.71	0.64	0.35	0.79	0.57	1.10	n.d.	n.d.	n.d.	n.d.	n.d.
G12	pale green	33.54	3.01	60.40	0.57	0.64	0.55	0.48	0.81	n.d.	n.d.	n.d.	n.d.	n.d.
G12	dark green	33.55	3.41	59.16	n.d.	0.50	0.68	0.82	0.86	n.d.	n.d.	1.06	n.d.	n.d.
K1	green	32.82	5.89	51.94	0.64	0.99	2.46	1.55	1.66	0.40	n.d.	1.75	n.d.	n.d.
K2	green	30.30	7.10	58.81	n.d.	0.98	n.d.	n.d.	1.36	n.d.	n.d.	1.22	n.d.	n.d.
K3	green	30.39	7.62	58.40	n.d.	0.97	n.d.	n.d.	1.57	n.d.	n.d.	0.75	n.d.	n.d.
K4	blue	39.61	2.41	44.27	1.86	1.43	2.50	0.75	0.42	n.d.	n.d.	n.d.	n.d.	6.76
K4	green	38.13	4.34	50.76	n.d.	0.79	1.46	0.81	1.64	n.d.	n.d.	2.08	n.d.	n.d.
K5	creamy white	55.34	1.64	30.82	7.79	1.06	1.86	0.74	0.76	n.d.	n.d.	n.d.	n.d.	n.d.
K5	blue	57.08	2.11	28.84	9.43	1.12	0.94	0.47	n.d.	n.d.	n.d.	n.d.	n.d.	n.d.
K6	yellow	29.75	4.89	62.83	n.d.	0.65	0.72	0.45	0.71	n.d.	n.d.	n.d.	n.d.	n.d.
K6	pale green	30.90	4.93	59.50	n.d.	0.88	0.80	0.35	0.82	n.d.	n.d.	1.82	n.d.	n.d.
K6	dark green	30.96	4.58	59.07	n.d.	0.71	0.72	0.66	1.24	n.d.	n.d.	2.06	n.d.	n.d.

n.d.: Not detected or below the detection limits.

Fig. 1. The plot of the quantities of PbO versus Na<sub>2</sub>O+K<sub>2</sub>O (wt%).

in the production of lead glazed layers of 18 lead glazed potsherds from the Ayasuluk region in İzmir.

## 2. Materials and methods

Representative optical images and macro descriptions of the lead glazed potsherds investigated in the study are given in Table 1.

### 2.1. Microstructural and microchemical characterization

Eighteen lead glazed potsherds were cut to obtain body-glaze cross-sectional samples. The samples were mounted with the vacuum impregnation method and polished to have flat surfaces prior to SEM investigation. Then, they were examined uncoated in a variable pressure field emission gun SEM (Zeiss Supra 50VP) attached with an energy dispersive X-ray

(EDX-Oxford Instruments) spectrometer under 20 kV with 8 mm working distance (WD).

## 2.2. Micro-Raman spectroscopy

The Raman spectra of the glazes were recorded in situ, in the  $100\text{--}2000\text{ cm}^{-1}$  region, using a micro-Raman multichannel spectrometer, (LabRam 300 Horiba Jobin-Yvon) equipped with doubled-frequency Nd:YAG laser operating at 532 nm and with an excitation power of around 5 mW at the sample. An Olympus MPlan microscope, with magnification of  $50\times$  and  $50\times$  LWD was used to focus the laser onto the sample.

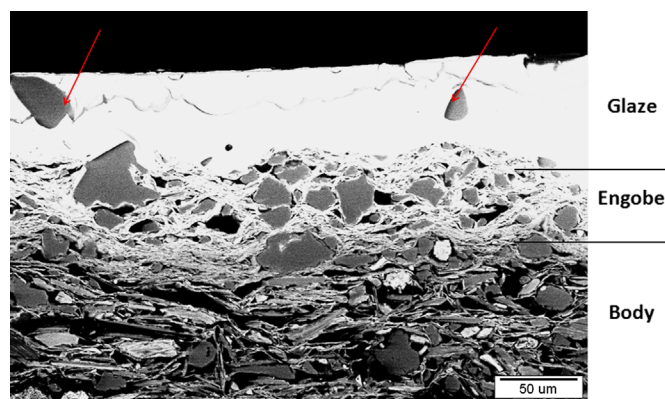


Fig. 2. Representative cross-sectional BSE image of sample G9 showing; glaze, engobe and body layers (arrows indicate residual quartz grains).

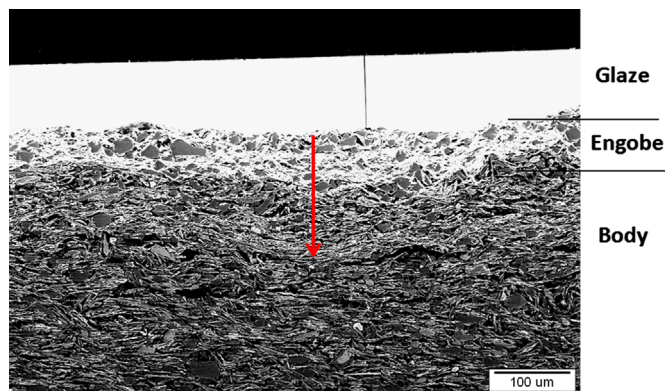


Fig. 3. Representative cross-sectional BSE image of sample G12 showing; glaze, engobe and body layers (arrow indicates lead oxide penetration into the body).

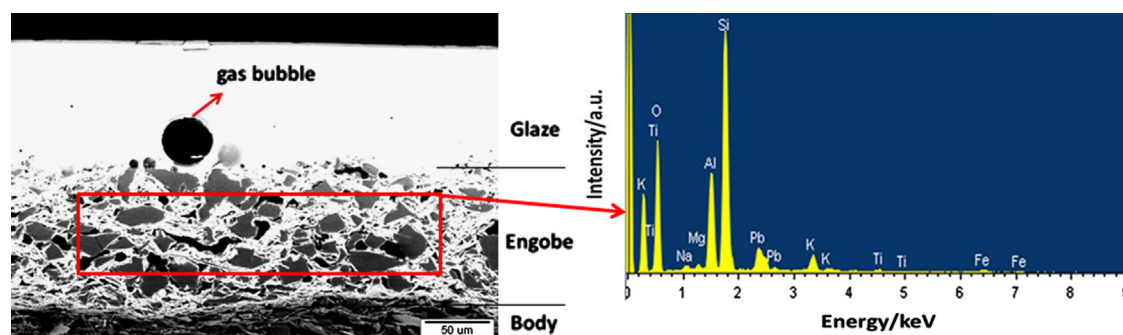


Fig. 4. Representative cross-sectional BSE image of sample K6 and the SEM-EDX spectrum of the silicate rich engobe layer.

The backscattered light was dispersed using 1800 lines/mm grating. The spectral resolution was around  $3\text{ cm}^{-1}$ . Acquisition times were between 5 and 10 s, with 10–20 scans. The laser diameter on the sample was  $2\text{ }\mu\text{m}$ . The LABSPEC package [6] was used for spectra acquisition and GRAMS 32 for spectra manipulation [7]. All the spectra were baseline corrected and filtered if needed by LABSPEC software to remove the background fluorescence and excessive noise.

## 3. Results and discussion

### 3.1. Microstructural and microchemical characterization

Semi-quantitative EDX analyses taken from different parts of the glazes are given in Table 2. As seen, the most prominent component in the glaze is PbO. Its amount changes between 49.09 and 72.89 wt% for most of the samples. The exceptions are four cases (K4, K5 and G10, G11) with relatively lower amounts between 24 and 40 wt% PbO. The amount of Na<sub>2</sub>O is in the range from 0.24 to 1.8 wt% for all the samples except for K5 where it reaches 9.43 wt%. The amount of K<sub>2</sub>O is in a moderate range from 0.25 to 3.20 wt%. CaO and MgO amounts are also in a moderate range from 0.45 to 2.50 wt% and 0.33 to 1.57 wt%, respectively. The plot of Na<sub>2</sub>O + K<sub>2</sub>O amounts versus that of PbO is given in Fig. 1 where the glaze types can be classified into two groups: most of the glazes were identified as transparent high lead glazes (related to the samples with PbO and alkali content). However, the glaze compositions of four samples (G10, G11, K4 and K5) can be defined as lead-alkali glazes. Transparent high lead glazes contain 45–60 wt% PbO, alkali oxides (Na<sub>2</sub>O + K<sub>2</sub>O) less than 2 wt% and 2–7 wt% Al<sub>2</sub>O<sub>3</sub>. This type glaze was extensively used throughout the Islamic and Byzantine empires, in the Medieval Europe for both pottery and tiles, and continuing to the present day in both Europe and the Near East [5].

Another type of lead glazes is tin-opacified glazes and first produced in eighth century in Iraq, but these were initially alkali glazes containing only 1–2 wt% PbO. Then, with the increasing lead content of these glazes up to 20–40 wt% PbO until the tenth and eleventh century, they were true lead-alkali glazes with higher amounts of alkali (5–12 wt%). Throughout the Near East and Europe, lead-alkali type glazes were used almost for all the production of tin-opacified glazes. However,



in Spain and in early Italian majolica, higher amounts of PbO (up to 55 wt%) with lower alkali contents (about 3 wt%) were used [5].

The dominant color of the glaze of potsherds is green, although brown, cream, yellowish and blue colors are also observed. An attempt was made to correlate the elemental composition of the analyzed potsherds with the glaze colors of the potsherds that appear in green, light green, yellow and brown.

The amount of iron oxide changes between 0.37 and 5.22 wt%, with the attributions to brown samples (G1–G4 and G7–G11), suggesting that iron oxides were used as coloring agents in these potsherds. The green colors in lead glazes are usually due to the presence of copper oxide as in G1, G2, G3, G6, G12, K1–K4, and K6 [8]. The amount of CuO in these samples changes between 0.61 and 3.94 wt%. But the pale green color under the glaze layer of the samples coded as K1, K2, K3, G1, and G10 and the dark green color under the glaze layer of the samples coded as K6, G3 and G12 should have been caused by the presence of CuO and iron oxide. However, the green color under the glaze layer of the samples coded as G1, G8, G9, G10 and G12 should have been generated by  $\text{Fe}^{2+}$  oxide combinations. Apart from the samples of G10 and G11, the yellow and brown colors under the glaze layers of the potsherds should have been provided by the presence of  $\text{Fe}^{3+}$  oxide and its combinations [9–11]. The blue color of the glaze of K4 sample may be arisen from the presence of FeO in the form of octahedral structure [11]. MnO gives purple and brown colors due to the proportions in relation to  $\text{Mn}^{2+}$  and  $\text{Mn}^{3+}$ . The presence of MnO may contribute to the brown color for the sample G10 [11,12]. Due to the high refractive index and small particle size of  $\text{SnO}_2$ , it should have also contributed to obtain opacity in the glaze of K4 sample [13–15].  $\text{TiO}_2$ , MnO,  $\text{P}_2\text{O}_5$  and  $\text{SnO}_2$  were detected sparsely in different glaze layers.

From the SEM images, thickness of the glaze layers changes between 40 and 240  $\mu\text{m}$ . Almost all the samples have also interaction layer between the glaze and the underlying body (Figs. 2–4). In some of the interaction layers, the formation of potassium lead aluminum silicate crystals  $[(\text{Pb},\text{K})\text{AlSi}_3\text{O}_8]$  grown into the glaze layer was detected (Fig. 5). Production of lead glazed potteries using non-calcareous and calcareous clays results in different types of crystals at the glaze/body

interface. Wollastonite crystals are formed in the glaze/body interface instead of lead-feldspars with calcareous clays during firing. The thickness of these crystal layers may indicate the firing temperature of potteries [1]. There are parameters controlling the sluggish diffusion processes into the glaze layer of the underlying body for the formation of interaction layers. These parameters are peak firing temperature, soaking time, viscosity of the glaze layer during firing, chemical and phase content of the glaze and body layers. Therefore, the chemical composition of interaction layers may change in a wide range of elements and quantities [16]. Some residual quartz grains inside the glaze layers were also observed (Fig. 2). The round shape of these grains indicates high temperature of melting. Translucent, bright and durable lead glazes in such compositions can be obtained in a temperature range from 700 to 800  $^{\circ}\text{C}$  [17]. There are two primary methods of producing a lead glaze. They are either applied as lead oxide (or some other lead compounds) to the surface of the pottery body, or as a mixture of lead oxide with quartz. A small amount of clay can be included in the glaze slurry, and the application can be either unfired or biscuit fired bodies with both methods [1].

Gas bubbles were observed in some of the investigated glazes (Figs. 4 and 6). They might have been caused due to the burning of the organic materials, which were used for adhering purposes in the past, in the glazes. Although the gas bubbles

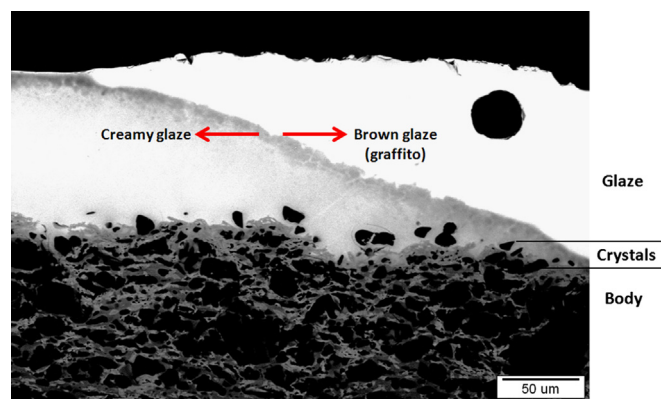


Fig. 6. Representative cross-sectional BSE image of sample G11 showing the contrast difference between creamy white glaze layer and brown graffito application.

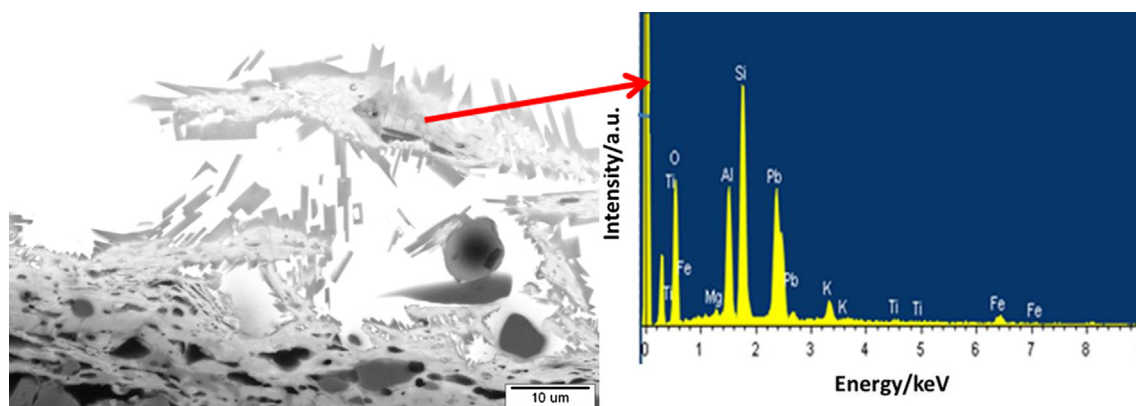


Fig. 5. Representative cross-sectional BSE image of the glaze-body interaction layer of K3 and the SEM-EDX spectrum of the rod-shaped interface crystals.

grow in the glaze, they could not reach to the surface of the glaze, due to the high viscosity of the glazes [18]. Considering microstructural and microchemical characteristics of the investigated glaze layers, it may be suggested that both types of glaze production were performed for the potteries from Smyrna [1].

### 3.2. Micro-Raman spectroscopy

Micro-Raman spectroscopy is an efficient tool for non-destructive analysis of silicate glasses. Based on the position and intensities of Si–O stretching and bending mode in the Raman spectrum, the processing temperature could be estimated [17,19–22]. Two main features are observed in the Raman spectra of silicate glasses: one between 300 and 600  $\text{cm}^{-1}$  corresponding to Si–O–Si bending vibrations within intertetrahedron linkages and the other between 900 and 1300  $\text{cm}^{-1}$  associated with Si–O stretching vibrations. Colom-ban et al. [17,19–22] have shown that the degree of polymerization of  $\text{SiO}_4$  units can be quantitatively expressed by polymerization index  $I_p$ , defined as the ratio of the bending and stretching envelope areas,  $A_{500}/A_{1000}$ . Lead oxide added as a flux agent breaks down Si–O links leading to structures characterized by isolated and poorly connected tetrahedral

units. In all the analyzed Raman spectra, the intensity of the Si–O stretching mode envelope (between 850 and 1100  $\text{cm}^{-1}$ ) is much higher compared to bending Si–O–Si mode envelope (around 500  $\text{cm}^{-1}$ ). Medieval ceramics, from Turkey (Islamic glazes [17,19,20]) and the Balkans (Byzantine glazed ceramics [21,23,24]) have been characterized by such features in the Raman spectra. In the spectra of the glazes with higher amount of lead oxide, the center of the stretching band is shifted to lower wavenumbers as a result of the higher depolymerization of Si–O network and formation of less compact structure characterized by lower polymerization index (Fig. 7a). The results of the calculated polymerization indexes on the analyzed glazes are given in Fig. 7b. As seen from Fig. 7c, the obtained  $I_p$  values are low, ranging between 0.04 and 0.24, characteristic to lead rich glazes. The samples K5 and G11 did not yield useful spectra by the Raman spectroscopy due to corroded nature of their glazes. Based on the EDX results, these two samples were estimated as alkali-lead glazes with much lower PbO and higher alkali content. It should be noted that lead rich glazes were believed to be about 700 °C.

Investigated glazes are distinctly colored in green, brown, yellow and cream. The coloration of the glazes is obtained using different mineral pigments, yet it was quite difficult to

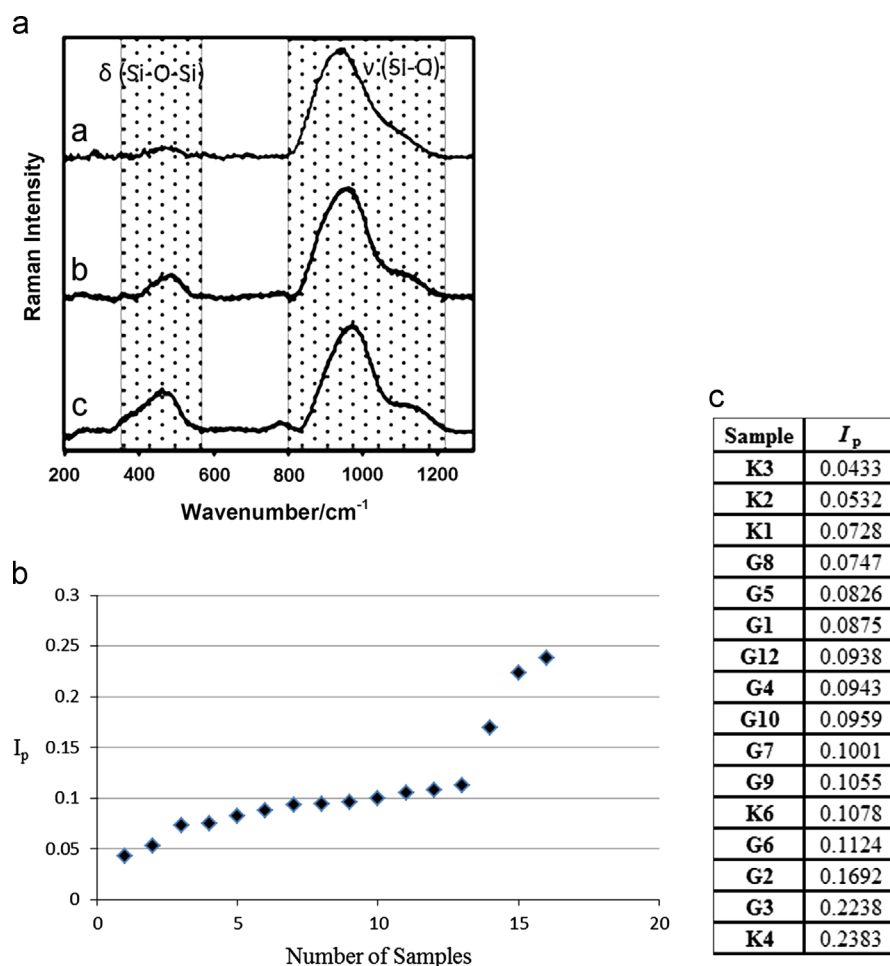


Fig. 7. (a) Representative Raman spectra of some samples with different polymerization indexes ( $I_p$ ): a—K3 ( $I_p=0.043$ ); b—G7 ( $I_p=0.100$ ) and c—K4 ( $I_p=0.238$ ), (b) cumulative graph of calculated  $I_p$  values for the investigated samples and (c)  $I_p$  values, used in (b).

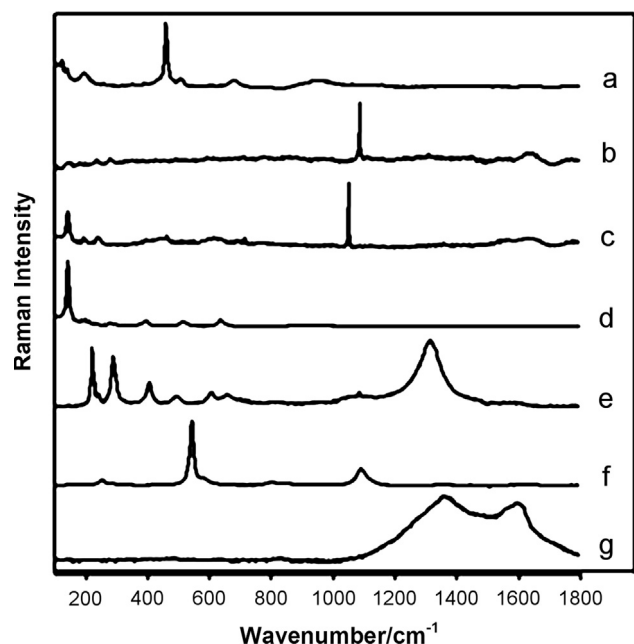


Fig. 8. Raman spectra of pigments identified in the ceramic glaze: a—quartz; b—calcite; c—lead white and anatase; d—anatase; e—red ochre; f—lazarite; and g—carbon black.

identify them in the Raman spectra since they were dissolved in the glassy matrix. Several mineral pigments, however, were identified: lead white, anatase, quartz, calcite, red ochre, lazurite and carbon black (Fig. 8). Although some of them are common constituents of clays, their connection with the obtained color of the glaze show that they were added on purpose, to obtain desired color (white, creamy, yellow to brown and blue). In the case of green colored glazes, although copper was identified by SEM-EDX, no mineral pigment related to copper was identified by Raman spectroscopy.

#### 4. Conclusions

The results showed that lead-rich glazes should have been prepared and applied on quartz-rich engobe layer of the ceramic bodies. SEM images showed the presence of rod-shaped crystals formed between body and glaze layers due to the interaction of the body and glaze during firing. Round shape of residual grains in the glaze layers and lead-rich feldspar arrangements at the interaction layers indicate high temperature firing. Low polymerization indexes ( $I_p$ ) of the glazes calculated by micro-Raman analysis indicated that all the glazes might have been fired at around 700 °C. It is obvious that copper and iron oxides were the main colorants while manganese and tin oxides were rarely used for decorations. It may be considered that the concentration and firing atmosphere of these oxides were the main parameters to obtain different color shades and effects.

#### Acknowledgments

Financial support by the Scientific and Technological Research Council of Turkey (TÜBİTAK) with the Project no. 108M386

and Ministry of Education and Science, Republic of Macedonia Macedonian–Turkish bilateral Project titled “Byzantine and Early Ottoman Artifacts (Ceramics and Metal Objects) in Republic of Macedonia and Turkey: Characterization and Comparison” is acknowledged.

#### References

- [1] M.S. Walton, M.S. Tite, Production technology of Roman lead-glazed pottery and its continuance into late antiquity, *Archaeometry* 52 (2010) 733–759.
- [2] K. Greene, Late hellenistic and early Roman invention and innovation: the case of lead-glazed pottery, *Am. Journal of Archaeology* 111 (2007) 653–671.
- [3] A.P. Kazhdan, A.W. Epstein, *Change in Byzantine Culture in the Eleventh and Twelfth Centuries*, University of California Press, London 70–71.
- [4] G. Simsek, P. Colomban, V. Milande, Tentative differentiation between Iznik tiles and copies with Raman spectroscopy using both laboratory and portable instruments, *Journal of Raman Spectroscopy* 41 (2009) 529–536.
- [5] M.S. Tite, I. Freestone, R. Mason, J. Molera, M. Vendrell-Saz, N. Wood, Lead glazes in antiquity—methods of production and reasons for use, *Archaeometry* 40 (1998) 241–260.
- [6] LabSpec, Version 5.25.15, 2007.
- [7] Galactic Industries Corporation, GRAMS/32 Spectral Notebook Version 4.10, 1996.
- [8] S. Paynter, F. Okyar, S. Wolf, M.S. Tite, The production technology of Iznik pottery—a reassessment, *Archaeometry* 46 (2004) 421–437.
- [9] A.C. Charalambous, A.J. Sakalis, N.A. Kantiranis, L.C. Papadopolou, N.C. Tsirliganis, J.A. Stratis, Cypriot Byzantine glazed pottery: a study of the Paphos workshops, *Archaeometry* 52 (2010) 628–643.
- [10] J. Molera, M. Vendrell-Saz, M. Garcia-Valles, Technology and colour development of Hispano–Moresque lead-glazed pottery, *Archaeometry* 39 (1997) 23–39.
- [11] S.S. Ramos, F.B. Reig, J.V.G. Adelantado, D.J.Y. Marco, A.D. Carbó, Study and dating of medieval ceramic tiles by analysis of enamels with atomic absorption spectroscopy, X-ray fluorescence and electron probe microanalysis, *Spectrochimica Acta Part B* 57 (2002) 689–700.
- [12] M.S. Tite, Y. Maniatis, D. Kavoussanaki, M. Panagiotaki, A.J. Shortland, S.F. Kirk, Colour in Minoan faience, *Journal of Archaeological Science* 36 (2009) 370–378.
- [13] R.B. Mason, M.S. Tite, The beginnings of tin-opacification of pottery glazes, *Archaeometry* 39 (1997) 41–58.
- [14] M. Vendrell, J. Molera, M.S. Tite, Optical properties of tin-opacified glazes, *Archaeometry* 42 (2000) 325–340.
- [15] J. Molera, T. Pradell, N. Salvadó, M. Vendrell-Saz, Evidence of tin oxide recrystallization in opacified lead glazes, *Journal of the American Ceramic Society* 82 (1999) 2871–2875.
- [16] A. Kara, R. Stevens, Interactions between an ABS type leadless glaze and a biscuit fired bone china body during glaze firing. Part II: investigation of interactions, *Journal of the European Ceramic Society* 22 (2002) 1103–1112.
- [17] P. Colomban, W. Milande, L. Le Bihan, On-site Raman analysis of Iznik pottery glazes and pigments, *Journal of Raman Spectroscopy* 35 (2004) 527–535.
- [18] R. Padilla, O. Schalm, K. Janssens, R. Arrazcaeta, P. Van Espen, Microanalytical characterization of surface decoration in Majolica pottery, *Analytica Chimica Acta* 535 (2005) 201–211.
- [19] P. Colomban, F. Treppoz, Identification and differentiation of ancient and modern European porcelains by Raman macro- and micro-spectroscopy, *Journal of Raman Spectroscopy* 32 (2001) 93–102.
- [20] P. Colomban, Polymerization degree and Raman identification of ancient glasses used for jewellery, ceramics enamels and mosaics, *Journal of Non-Crystalline Solids* 323 (2003) 180–187.



- [21] P. Colomban, R. de Laveaucoupet, V. Milande, On-site Raman spectroscopic analysis of Kütahya fritwares, *Journal of Raman Spectroscopy* 36 (2005) 857–863.
- [22] P. Colomban, A. Tournie, L. Bellot-Gurlet, Raman identification of glassy silicates used in ceramics, glass and jewellery: a tentative differentiation guide, *Journal of Raman Spectroscopy* 37 (2006) 841–852.
- [23] V. Tanevska, P. Colomban, B. Minčeva-Šukarova, O. Grupče, Characterization of pottery from Republic of Macedonia I: Raman analysis of Byzantine glazed pottery, excavated from Prilep and Skopje (12th–14th century), *Journal of Raman Spectroscopy* 40 (2009) 1240–1248.
- [24] A. Raškovska, B. Minčeva-Šukarova, O. Grupče, P. Colomban, Characterization of pottery from Republic of Macedonia II. Raman and infrared analyses of glazed pottery finds from Skopsko Kale, *Journal of Raman Spectroscopy* 41 (2010) 431–439.